



## **NEW INFORMATION ABOUT INCREMENTAL STRAIN METHOD USED FOR RESIDUAL STRESS MEASUREMENT BY RING-CORE METHOD**

**A. Cívín\*, M. Vlk\***

**Summary:** *This paper follows up an article Analysis of Calibration Coefficients of Incremental Strain Method Used for Residual Stress Measurement by Ring-Core Method (Cívín, 2010), where the values of the calibration coefficients  $K_1$  and  $K_2$  have been determined in dependence on the depth of drilled hole and on the disposition of the residual state of stress. Influence of blunting the cutting tool during drilling process is taken into account and new calibration coefficients are compared with the common ones, which are determined without radius at the bottom of the annular groove. Evaluation of relaxed strains by integration across the strain gauge's measuring grid is considered too.*

### **1. Introduction**

The ring-core method is the semi-destructive experimental method used for the evaluation of homogeneous and non-homogeneous residual stresses, acting over depth of drilled core. Therefore, the specimen is not totally destroyed during measurement and in many cases could be used for another application.

One of the applicable theory which is based on the procedure of evaluating magnitude of the residual stress is called the incremental strain method. On the one hand, despite its great theoretical shortcoming which assumes that the measured deformations  $d\varepsilon_x$  and  $d\varepsilon_y$  are functions only of the residual stresses acting in the current depth  $z$  of drilled hole and do not depend on the previous increments  $dz$  and residual stresses, this method is still often used. On the other hand, relieved strains do not depend only on the stress acting within drilled layer but also on the geometric changes of the ring groove during deepening. In consequence of this, relaxations of strains is still continuing and grooving with drilled depth even if next step increment contains no residual stress. For this reason, proposed theory purveys only approximate information about real state of stress.

This paper follows up an article Analysis of Calibration Coefficients of Incremental Strain Method Used for Residual Stress Measurement by Ring-Core Method (Cívín, 2010), where the values of the calibration coefficients  $K_1$  and  $K_2$  have been determined in dependence on the depth of drilled hole and on the disposition of applied uniaxial and biaxial residual stress state. New progress has been made towards to the achievement of more believable finite element model by taking into account influence of cutting tool's blunting. In addition, comparison of evaluated calibration coefficients calculated from relieved strains in the middle

\* Ing. Adam Cívín, doc. Ing. Miloš Vlk, CSc.: Institute of Solid Mechanics, Mechatronics and Biomechanics, Brno University of Technology, Technická 2896/2, 616 69 Brno, Czech Republic, e-mails: [civin.adam@seznam.cz](mailto:civin.adam@seznam.cz); [vlk@fme.vutbr.cz](mailto:vlk@fme.vutbr.cz)

point and across the strain gauge's measuring grid has been considered too.

Investigation of influence on magnitude of relieved strains and subsequent determination of the calibration coefficients  $K_1$  and  $K_2$  for various thickness of FE-model is interesting to consider too (Civín, 2009).

## 2. Problem description

The biaxial residual stress state occurs more frequently in mechanical parts rather than the uniaxial residual stress state. For this reason should be our attention aimed to study influence on evaluation of calibration coefficients  $K_1$  and  $K_2$  caused by changing geometry of the ring groove under biaxial state of stress conditions in comparison with uniaxial state of stress certainly. That means how much are values of these calibration coefficients affected by changing geometry of the annular groove's bottom, caused by blunting of the cutting tool. Attention should be paid to the way how are relieved strains  $\varepsilon_1$  and  $\varepsilon_2$  calculated, i.e. by using single value of relieved strain in the middle point of each gauge's measuring grid or by integration of relieved strains across whole strain gauge's measuring grid. Influence of model's thickness should be considered too.

### 2.1. Basic equations

In general, equations (1, 2) describe determination of principal stresses  $\sigma_1$  and  $\sigma_2$  calculated from measured strains  $\varepsilon_1$  and  $\varepsilon_2$  on the top surface of the core, where the three-element ring-core rosette is placed. With known magnitude of the calibration coefficient  $K_1$  and  $K_2$  and numerical derivation of relaxed strains  $d\varepsilon_1/dz$  and  $d\varepsilon_2/dz$  in dependence on the constant step of increment's magnitude  $dz = \text{const.} = 0.2 \text{ mm}$  could by residual stresses obtained by following equations:

$$\sigma_1 = \frac{E}{K_1^2 - \mu^2 K_2^2} \cdot \left( K_1 \frac{d\varepsilon_1}{dz} + \mu K_2 \frac{d\varepsilon_2}{dz} \right); \quad \sigma_2 = \frac{E}{K_1^2 - \mu^2 K_2^2} \cdot \left( K_1 \frac{d\varepsilon_2}{dz} + \mu K_2 \frac{d\varepsilon_1}{dz} \right) \quad (1, 2)$$

where  $E$  is Young's modulus,  $\mu$  is Poisson's ratio and  $d\varepsilon_1/dz$ ,  $d\varepsilon_2/dz$  are numerical derivations of relaxed strains

Formulations, suggested by equations (1, 2), have a problem. Because if the denominator  $K_1^2 - \mu^2 K_2^2$  becomes zero for certain values of  $K_1$  and  $K_2$ , the stress will become infinite. Further, equations (1, 2) are used to derive valid equations for uniaxial and biaxial state of stress.

#### Uniaxial state of stress:

Equations for calibration coefficients  $K_1$ ,  $K_2$  ( $\sigma_1 \neq 0, \sigma_2 = 0$ ):

$$K_1 = \frac{E}{\sigma_1} \cdot \frac{d\varepsilon_1}{dz}; \quad K_2 = -\frac{E}{\mu \sigma_1} \cdot \frac{d\varepsilon_2}{dz} \quad (3, 4)$$

#### Biaxial state of stress:

Equations for calibration coefficients  $K_1$ ,  $K_2$  obtained by modification of eq. (1, 2) for  $\sigma_1 \neq 0, \sigma_2 \neq 0$ :

$$K_1 = \frac{E}{\sigma_1(1-\kappa^2)} \cdot \left( \frac{d\varepsilon_1}{dz} - \kappa \frac{d\varepsilon_2}{dz} \right); \quad K_2 = -\frac{E}{\mu \sigma_1(1-\kappa^2)} \cdot \left( \kappa \frac{d\varepsilon_1}{dz} - \frac{d\varepsilon_2}{dz} \right) \quad (5, 6)$$

where  $\kappa = \frac{\sigma_2}{\sigma_1}$ . (7)

The formulations suggested by equations (5, 6) have a problem with denominator too. If  $\sigma_1 = \sigma_2$  or  $\sigma_1 = -\sigma_2$ , then  $(1 - \kappa^2)$  becomes zero and the stress will become infinite.

### 3. Results

Simulation by FEM is the only reasonable way how to obtain desired information or how to simulate real experiment. Analysis system called ANSYS is used for FE-simulation. FE-analysis is based on a specimen volume with dimensions of  $50 \times 50 \text{ mm}$  and thickness of  $50 \text{ mm}$ . Due to symmetry, only a quarter has been modeled with centre of the core on the surface as the origin. Shape of the model is simply represented by block with planar faces with quarter off drilled annular groove (Figures 1 and 2). The annular groove has been made by 40 increments with constant step size of  $dz = 0.2 \text{ mm}$ . Therefore, the full depth of drilled groove is  $z = 8 \text{ mm}$ . Dimension of outer diameter is  $18 \text{ mm}$  and width of annular groove is  $2 \text{ mm}$ . Figures 3 and 4 represent detail of FE-model without ( $R = 0 \text{ mm}$ ) and with ( $R = 0.5 \text{ mm}$ ) radius at the bottom of the annular groove. Linear, elastic and isotropic material model is used with material properties of Young's modulus  $210 \text{ GPa}$  and Poisson's ratio  $\mu = 0.3$ . Relaxed strains  $\varepsilon_1$  and  $\varepsilon_2$  have been measured at real positions of strain gauge rosettes' measuring grids in the middle point and by integration across its surface. Length and width of each measuring grid is  $5 \text{ mm}$  and  $1.9 \text{ mm}$  respectively.

Graphs of relaxed strains calculated across strain gauge's measuring grid, their numerical derivation and determined coefficients  $K_1$  and  $K_2$  are plotted in Figures 5 through 8 in case of uniaxial state of stress ( $\sigma_1 = 60 \text{ MPa}$ ,  $\sigma_2 = 0 \text{ MPa}$ ) and in case of biaxial state of stress ( $\sigma_1 = 60 \text{ MPa}$ ,  $\sigma_2 = 30 \text{ MPa}$ ) in Figures 9 through 12. Influence of constant radius  $R = 0.5 \text{ mm}$  (R0.5) and constantly increasing dimension of radius  $R = 0 \div 0.5 \text{ mm}$  (R\_var) with increment  $0.5/40 = 0.0125 \text{ mm}$  per one drilling step  $dz = \text{const} = 0.2 \text{ mm}$  has been compared with model without radius (R0) for these two types of stress state.

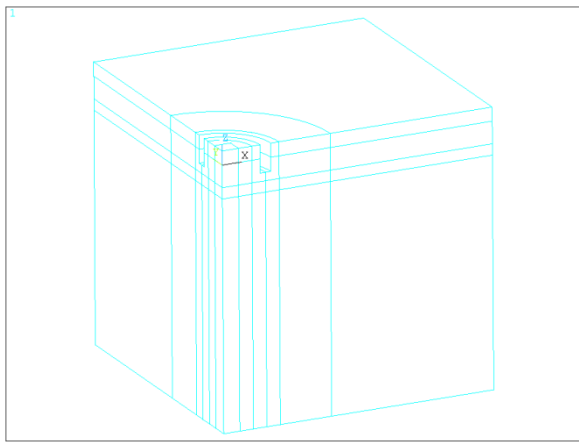


Figure 1 Quarter of global model

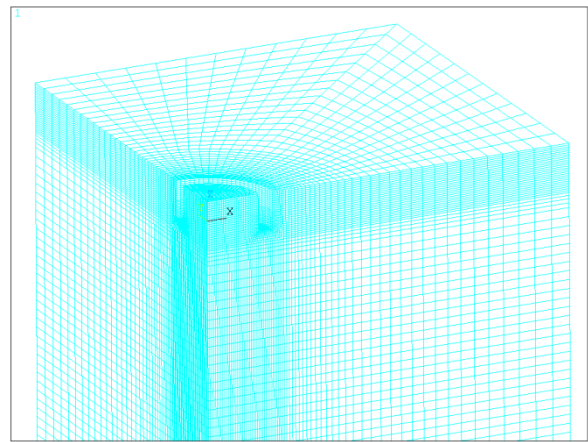


Figure 2 Model's global finite element mesh

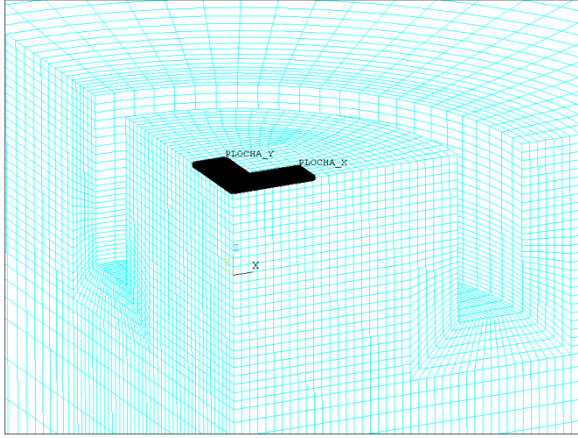


Figure 3 Detail of FE-mesh with  $R = 0$  mm

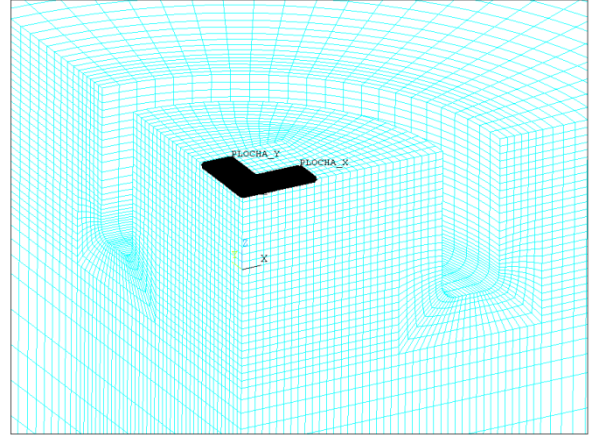


Figure 4 Detail of FE-mesh with  $R = 0.5$  mm

Points in Figures 13 through 16 show influence of relieved strains measured in the middle point of strain gauge's measuring grid (e.g.  $\epsilon_{1(z)}_{\text{point}}$ ) vs. measured strains integrated across measuring grid (e.g.  $\epsilon_{1(z)}_{\text{int}}$ ) in case of uniaxial state of stress. Drilled annular groove is considered without any radius.

Graphs, representing influence of model's thickness for various dimensions of  $t = 10$  mm (T10),  $t = 50$  mm (T50) and  $t = 100$  mm (T100), with respect to preservation of all other dimension are shown in Figures 19 through 22. All simulations have been done only for uniaxial state of stress ( $\sigma_1 = 60$  MPa,  $\sigma_2 = 0$  MPa) and with no radius at the annular groove's bottom.

### 3.1. Uniaxial state of stress

Values of relieved strains are measured by integration across strain gauge's measuring grid with simulated homogenous residual stress state ( $\sigma_1 = 60$  MPa,  $\sigma_2 = 0$  MPa). Magnitudes of the calibration coefficients are calculated using equations (3, 4). Influence of radius existence on the calibration coefficients ( $K_1$  and  $K_2$ ) determination inside the groove seems to be minimal, but no insignificant (Figures 7 and 8). For this reason should be paid attention to consider influence of cutting tool's blunting in all further simulations to minimize inaccuracy of the residual stress determination.

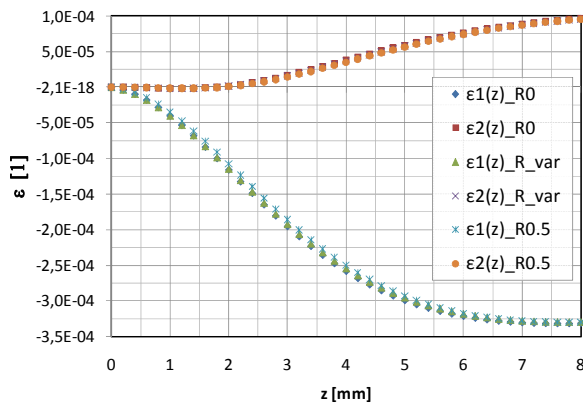


Figure 5 Relieved strains for uniaxial stress state

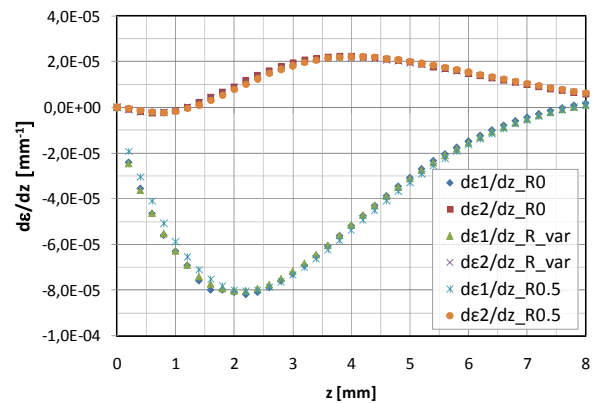


Figure 6 Numerical derivation of relieved strains

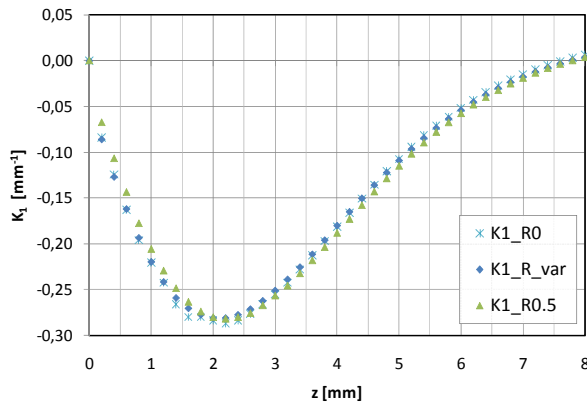


Figure 7 Calibration coefficient  $K_1$  for uniaxial residual stress state

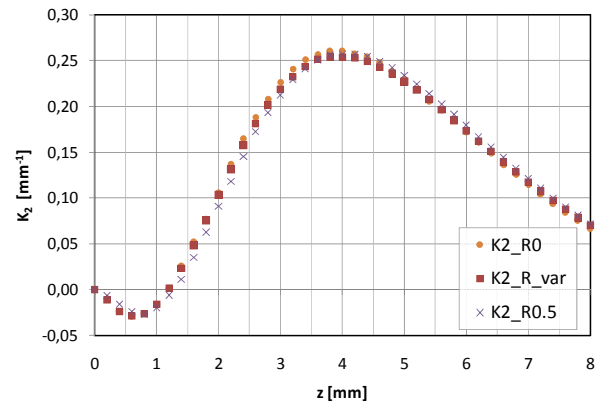


Figure 8 Calibration coefficient  $K_2$  for uniaxial residual stress state

### 3.2. Biaxial state of stress

Values of relieved strains are measured by integration across strain gauge's measuring grid with simulated homogenous residual stress state ( $\sigma_1 = 60 \text{ MPa}$ ,  $\sigma_2 = 30 \text{ MPa}$ ). Magnitudes of the calibration coefficients are calculated using equations (5, 6).

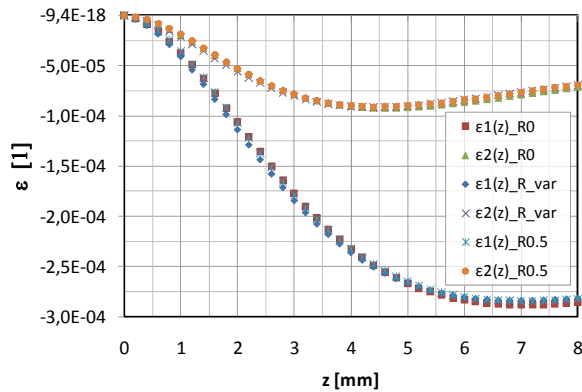


Figure 9 Relieved strains for biaxial stress state

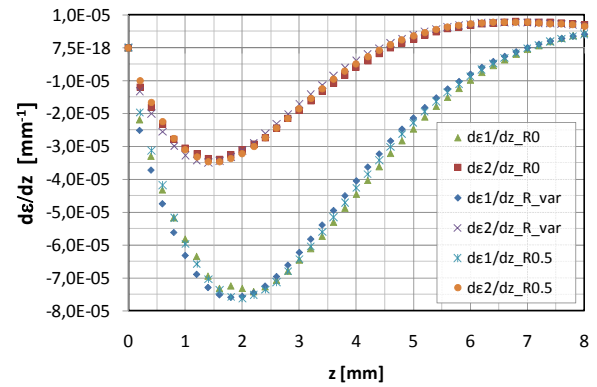


Figure 10 Numerical derivation of relieved strains

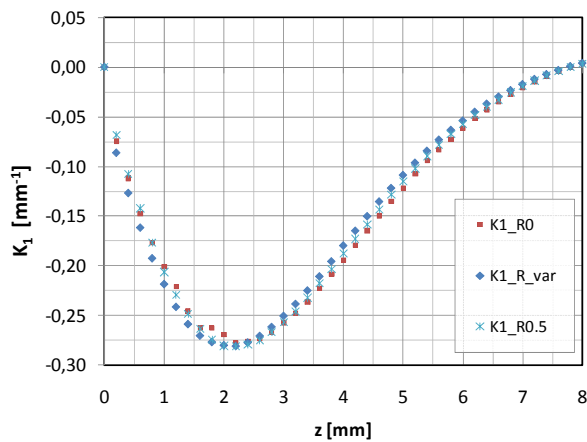


Figure 11 Calibration coefficient  $K_1$  for biaxial residual stress state

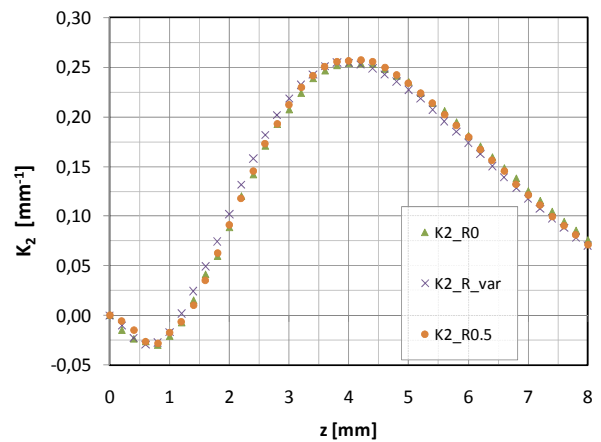


Figure 12 Calibration coefficient  $K_1$  for biaxial residual stress state

Influence of radius existence on the calibration coefficients ( $K_1$  and  $K_2$ ) determination inside the groove (Figures 11 and 12) is the same like for the uniaxial stress state simulation. For this reason, influence of cutting tool's blunting in all further simulations should be considered too.

### 3.3. Measuring grid's evaluation

Interesting is to observe behavior of the calibration coefficients  $K_1$  and  $K_2$  determined by using either the single value of relieved strains  $\varepsilon_1$  and  $\varepsilon_2$  in the middle point of each gauge's measuring grid (e.g.  $\varepsilon_{1(z)}_{\text{point}}$ ) or by integration of relieved strains across whole strain gauge's measuring grid (e.g.  $\varepsilon_{1(z)}_{\text{int}}$ ). Uniaxial state of stress ( $\sigma_1 = 60 \text{ MPa}$ ,  $\sigma_2 = 0 \text{ MPa}$ ) has been used for model with no radius at the bottom of the annular groove.

Points, representing calculated coefficients (Figures 15 and 16), show that measuring of relieved strains in the middle point of the strain gauge's measuring grid gives smaller values of the calibration coefficient  $K_1$  till the depth of drilled groove  $z = 2.8 \text{ mm}$  and slightly great values for depth larger than  $z = 2.8 \text{ mm}$ . In case of the calibration coefficient  $K_2$  is this influence vice versa till the depth of  $z = 4.6 \text{ mm}$ .

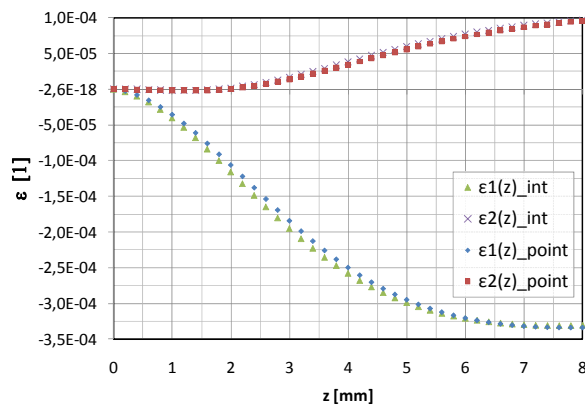


Figure 13 Relieved strains for uniaxial stress state and zero radius (R0)

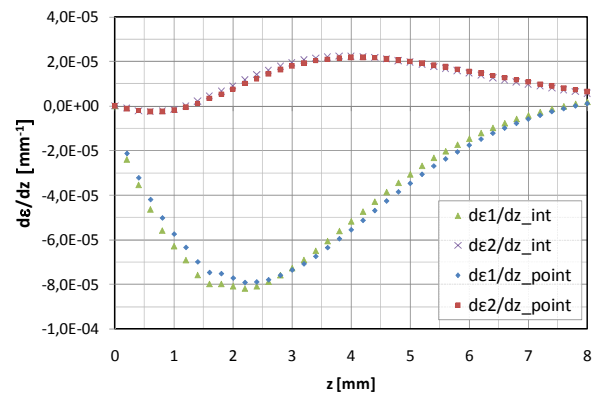


Figure 14 Numerical derivation of relieved strains

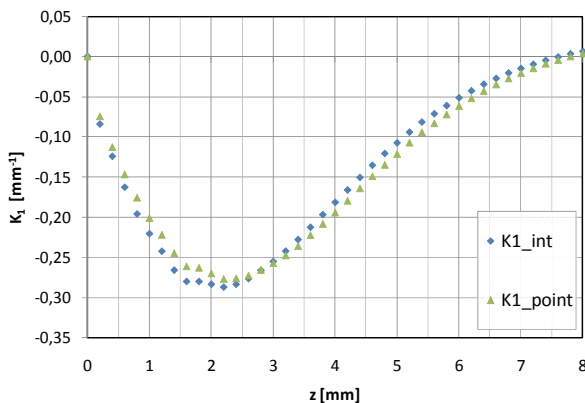


Figure 15 Calibration coefficient  $K_1$  for uniaxial stress state and zero radius (R0)

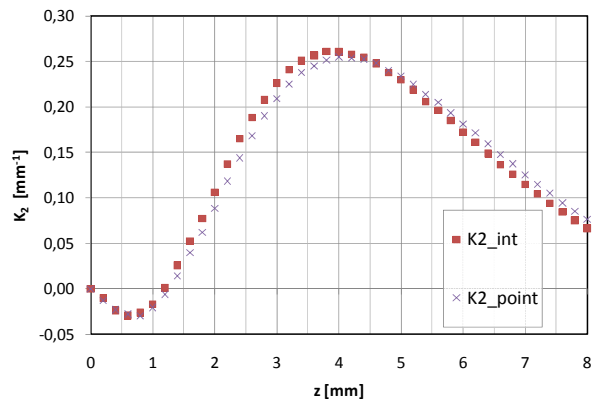


Figure 16 Calibration coefficient  $K_2$  for uniaxial stress state and zero radius (R0)

Differences (in percent) of the calibration coefficients'  $K_1$  and  $K_2$  values calculated in the middle point of strain gauge's measuring grid from the ones, calculated by integration across

measuring grid with respect to values measured by integration across measuring grid, are plotted in Figures 16 and 17 respectively. The greatest differences are for the calibration coefficient  $K_1$  for all depths from  $z = 6 \text{ mm}$  and for the calibration coefficient  $K_2$  till the depth of  $z = 1.8 \text{ mm}$ . Minimum difference between values  $K_1$  and  $K_2$  calculated in the middle point of strain gauge's measuring grid and values calculated by integration across measuring grid occurs in the depth of  $z = 2.8 \text{ mm}$  and  $z = 4.6 \text{ mm}$  respectively.

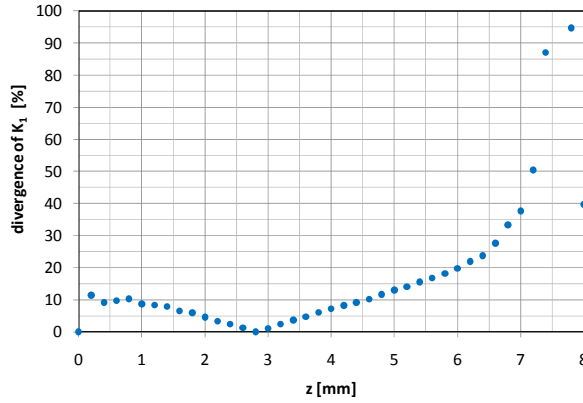


Figure 17 Divergence of  $K_1$  middle point values from values integrated across measuring grid

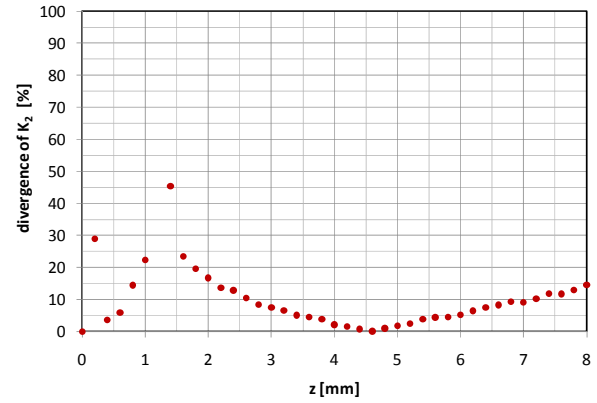


Figure 18 Divergence of  $K_2$  middle point values from values integrated across measuring grid

### 3.4. Finite element model's thickness

Values of relieved strains are measured by integration across strain gauge's measuring grid with simulated homogenous residual stress state ( $\sigma_1 = 60 \text{ MPa}$ ,  $\sigma_2 = 0 \text{ MPa}$ ) and with no radius at the annular groove's bottom. Graphs with points, representing influence of model's thickness for various dimensions of  $t = 10 \text{ mm}$  (T10),  $t = 50 \text{ mm}$  (T50) and  $t = 100 \text{ mm}$  (T100) with respect to preservation of all other dimension are shown in Figures 19 through 22.

Numerical values of the calibration coefficient  $K_1$  don't seem to be noticeably affected by various model's thickness. But in case of the calibration coefficient's  $K_2$  determination has influence of thin model (T10) significant impact on the residual stress determination for the most important part of drilled depth till  $z = 3.6 \text{ mm}$ .

In general, assumption of the incremental strain method theory suppose annular groove to be drilled in a sufficient distance from model's geometrical boundaries. For this reason should be model's thickness of at least  $t = 50 \text{ mm}$  considered for any other simulations.

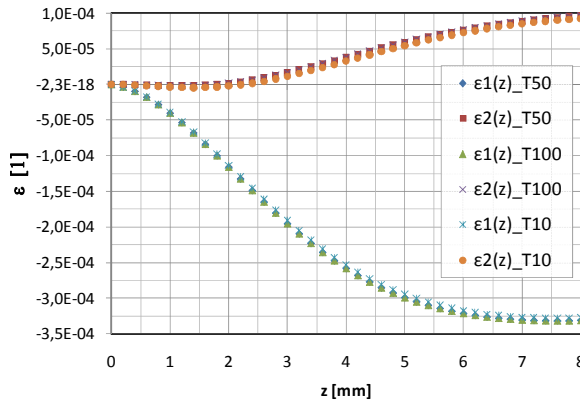


Figure 19 Relieved strains for uniaxial stress state

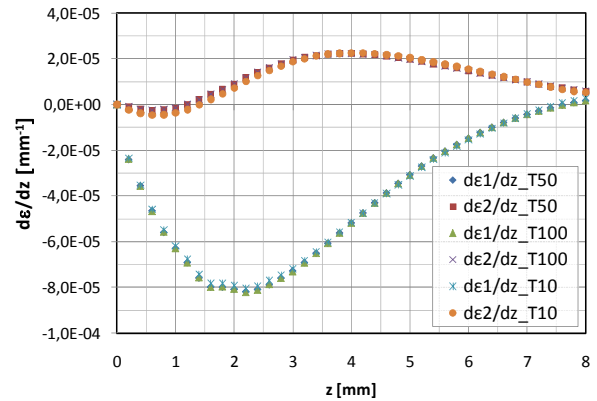


Figure 20 Numerical derivation of relieved strains



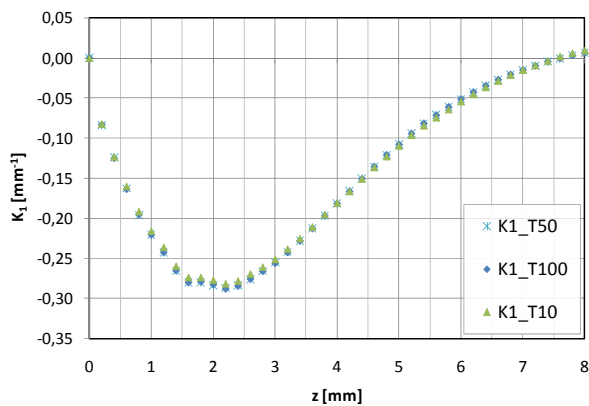


Figure 21 Calibration coefficient  $K_1$  for uniaxial stress state and zero radius (R0)

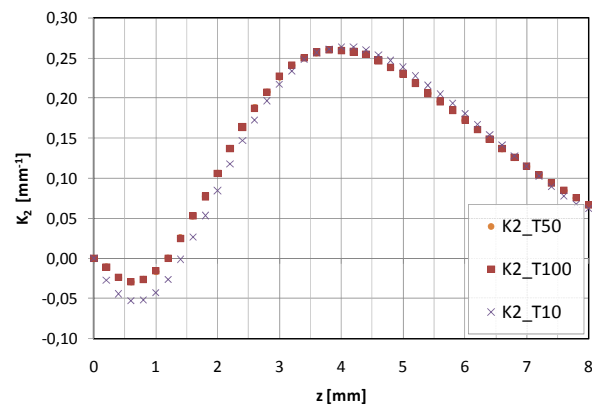


Figure 22 Calibration coefficient  $K_2$  for uniaxial stress state and zero radius (R0)

#### 4. Conclusion

This paper provides basic information about semi-destructive ring-core method. By using incremental strain method for residual state of stress determination, this article describes evaluation of the calibration coefficients  $K_1$  and  $K_2$  which are necessary for an analytical evaluation of principal residual stresses acting in every drilled layer.

Firstly, influence of changing magnitude of the annular groove's bottom radius, caused by blunting of the cutting tool, has been tested under uniaxial and biaxial state of stress.

In addition, differences of the calibration coefficients' values calculated in the middle point of strain gauge's measuring grid from the ones, calculated by integration across measuring grid have been tested under uniaxial stress state only.

Finally, influence of model's thickness has been considered and results gave important recommendations too.

Incremental strain method had been used frequently until the integral method has overcome its shortcomings. By concentrating the research on the observed weaknesses and the ambiguous details the ring-core method can be made an accurate and reliable method for residual stress measurement.

#### 5. References

- Civín, A.; Vlk, M.: (2010) Analysis of Calibration Coefficients For Incremental Strain Method Used for Residual Stress Measurement by Ring-Core Method. In: *Applied Mechanics 2010*, Jablonec nad Nisou,
- Civín, A.; Vlk, M.: (2009) Theoretical Analysis of Ring-Core Method for Residual Stress Determination. In: *Konference ANSYS 2009*, Plzeň, pp.205-212.
- Bohdan, P.; Holý, S.; Jankovec, J.; Jaroš, P.; Václavík, J.; Weinberg, O.: (2008) Residual stress measurement using ring-core method. In: *46. konf. Experimentální analýza napětí*, Horní Bečva,
- Keil S.: (1995) On-line evaluation of measurement results during the determination of residual stress using strain gages, *RAM*, Vol. 9, No. 1, pp. 15-20